Genotoxic interaction between deoxynivalenol and acrylamide

Chloé Huertas, Aboubacar B Coulibaly, Delphine Payros, Marie Penary, Sylvie Puel, Claire Naylies, Gaëlle Payros, Yannick Lippi, Isabelle P. Oswald, Gladys Mirey, et al.

Food Research International 214 (2025) 116633

Contents lists available at ScienceDirect

Food Research International

journal homepage: www.elsevier.com/locate/foodres

Genotoxic interaction between deoxynivalenol and acrylamide

Chloé Huertas [a], Aboubacar B. Coulibaly [a], Delphine Payros [a], Marie Penary [b], Sylvie Puel [a], Claire Naylies [a], Gaëlle Payros [a], Yannick Lippi [a], Isabelle P. Oswald [a], Gladys Mirey [a], Julien Vignard [a,*]

[a] Toxalim, Université de Toulouse, INRAE, ENVT, EI-Purpan, Toulouse, France
[b] IRSD, Université de Toulouse, INSERM, INRAE, ENVT, Univ Toulouse III Paul Sabatier (UPS), Toulouse, France

ARTICLE INFO

Keywords:
Deoxynivalenol
Acrylamide
Genotoxicity
Toxic interaction
Transcriptomic
Chromosomal instability

ABSTRACT

Food safety represents a major global concern. Humans and animals are exposed to a broad spectrum of food contaminants, which implies probable cocktail effects. Around 80 % of the population is exposed to deoxynivalenol (DON), one of the most widespread mycotoxins mainly found in cereal products. DON has previously been shown to exacerbate DNA damage induced by various compounds, questioning on potential toxic interactions with genotoxic food contaminants. Among them, acrylamide, classified as probably carcinogenic to humans, is formed during cooking processes and commonly found in fried foods and cereal products. Considering that co-consumption of DON- and/or acrylamide-contaminated foods is highly probable, we evaluated their genotoxic interaction in a non-cancerous intestinal cellular model. Our data show that DON exacerbates the cytotoxic and genotoxic activities of acrylamide, assessed through the analysis of the DNA damage biomarker γH2AX and by comet assay. This was corroborated by transcriptomic analyzes pointing out enhanced DNA repair pathway under co-exposure. Of note, DON-mediated increase of acrylamide-induced DNA damage is not related to the apoptotic program. As a consequence of this genotoxic interaction, cells co-exposed to DON and acrylamide exhibit more important cell cycle defects and chromosomal instability, as evaluated by the chromosomal aberration assay. In conclusion, our work shows that DON exacerbates the genotoxicity of acrylamide, with repercussions on the maintenance of genetic stability, potentially implying an increased carcinogenic risk. These results therefore provide crucial information regarding food safety, given the high probability of co-contamination by DON and genotoxic agents such as acrylamide.

1. Introduction

Food safety represents a major health issue, particularly since we are co-exposed on a daily basis to numerous contaminants through diet. Mycotoxins, the most naturally occurring food contaminants worldwide, are detected in up to 60 to 80 % of food crops (Eskola et al., 2020). Trichothecenes produced by *Fusarium* species represent the largest group of mycotoxins. Among them, deoxynivalenol (DON) is the most widespread with the highest level of contamination, primarily found in human food and animal feed through contaminated cereals such as wheat, barley, oat or maize (Knutsen et al., 2017; Zhang et al., 2024). Contamination can occur at any stage of production, processing, transformation or storage, and greatly depends on agricultural practices and environmental factors such as temperature and humidity (Cinar & Onbaşı, 2020). Crop contamination by DON has been estimated around the world (Zhang et al., 2024). According to the European Food Safety Authority (EFSA), DON is detected in 44 % of cereals (EFSA, 2013). In China, DON is detected in 96.4 % of feed samples (Zhao et al., 2021). In United States, 75.7 % of corn grain and 88.2 % of corn silage are contaminated (Weaver et al., 2021), whereas DON is detected in 82 % of samples in Kenya (Kemboi et al., 2020). Bread represents a major source of DON contamination, as this food staple is consumed by billions of people and contributes to almost 10 % of energy intake worldwide. For instance, the average consumption of bread reaches 160 g per day for EU citizens (Ribet et al., 2024). Consequently, more than 94 % of individuals are exposed to DON at detectable levels, with a high dietary chronic exposure representing a health risk for approximately 12 % of the population (Namorado et al., 2024). These data question on potential toxic interactions with other dietary contaminants, defined as cocktail effects. In light of this, DON co-occurrence with other

* Corresponding author at: Toxalim (Research Centre in Food Toxicology), Université de Toulouse, INRA, ENVT, INP-Purpan, UPS, 31300 Toulouse, France.
E-mail address: julien.vignard@inrae.fr (J. Vignard).

https://doi.org/10.1016/j.foodres.2025.116633
Received 22 November 2024; Received in revised form 14 February 2025; Accepted 11 May 2025
Available online 13 May 2025

mycotoxins and their combined adverse effects have already been investigated (Alassane-Kpembi et al., 2017; Karsauliya et al., 2022). However, many different co-exposure scenarios involving other classes of food contaminants are highly plausible and still under-evaluated.

Among environmental pollutants representing a health risk to human, acrylamide has particularly drawn attention due to its widespread presence. While cigarette smoke and occupational exposure represent other important sources of acrylamide intoxication, this colorless and odorless organic compound also can contaminate food. Indeed, acrylamide is formed at temperatures above 120 °C by the Maillard reaction through frequently used cooking processes except boiling (Yan et al., 2023). Several factors influence the level of acrylamide in foodstuffs, including cooking parameters such as temperature and time, production and storage conditions of the raw material, or its chemical composition (EFSA CONTAM Panel, 2015). The Maillard reaction is a non-enzymatic chemical reaction between reducing carbohydrates and asparagine, more particularly occurring in coffee, potatoes and cereals products (Sarion et al., 2021). Thus, acrylamide is present in a wide variety of commonly consumed products, increasing the probability of co-exposure with other food contaminants.

DON thermal stability allows it to withstand high cooking and baking temperatures necessary for acrylamide formation. DON and acrylamide co-occurrence has been established in bakery products (Balbo & Woźniak, 2022) or more globally in grain (Thielecke & Nugent, 2018), and also observed in other types of food products such as beer (Bogdanova et al., 2018). More broadly, the co-consumption of foods contaminated with DON or acrylamide is highly conceivable regarding their prevalence and their presence in the same meal. Considering that DON and acrylamide represent public health risks, assessing their toxic interactions is an important issue that needs to be further investigated.

DON causes acute toxicity, gastrointestinal toxicity, immunotoxicity and hepatotoxicity, affecting animal and human health through many symptoms such as vomiting, diarrhea, abdominal pain or fever (Zhang et al., 2024). In the intestine, DON inhibits nutrients absorption, alters epithelium integrity, affects gut microflora, triggers inflammation and promotes chronic intestinal inflammatory diseases (Pinton & Oswald, 2014). DON toxicity arises from its capacity to bind and inhibit the peptidyl transferase center in the ribosome 60S subunit (Knutsen et al., 2017). This triggers a ribotoxic stress defined by both defective protein synthesis and induction of cellular stress responses, leading to oxidative stress, activation of related MAP kinases and their downstream pathways including inflammatory response, and mitochondrial dysfunction (Garofalo et al., 2025). Acrylamide exposure is associated to several toxic effects such as neurotoxicity, hepatotoxicity, developmental and reproductive toxicity, gastrointestinal tract dysfunction, immunotoxicity and genotoxicity (EFSA CONTAM Panel, 2015; Palus, 2024; Rifai & Saleh, 2020). Moreover, *in vivo* experimentation pointed out the carcinogenicity of acrylamide, therefore classified as a "probable human carcinogen" by the international Agency for Research on Cancer (IARC) (IARC, 1994). Cellular transformation of acrylamide to its reactive metabolite glycidamide results in the formation of covalent DNA adducts, considered to represent the route underlying the genotoxicity and carcinogenicity of acrylamide (EFSA CONTAM Panel, 2015). Indeed, the clastogenic and mutagenic properties of acrylamide and glycidamide have been extensively demonstrated *in vitro* and *in vivo*. However, the levels of dietary exposure to acrylamide do not clearly support a direct cancer risk for humans (Guth et al., 2023), although the margins of exposure do not exclude a concern (EFSA CONTAM Panel, 2015). In this context, identification of toxic interactions with other food contaminants could help improving risk assessment.

DON is not genotoxic and is classified as non-carcinogenic by IARC (Claeys et al., 2020). Though, data indicate that DON exacerbates DNA damage induced by several compounds generating different types of DNA lesions, among which the bacterial toxin colibactin associated with colorectal cancer and the fungicide captan (Garofalo, et al., 2023, Garofalo et al., 2022; Payros et al., 2017). These studies support that DON may potentiate the harmful effects of environmental genotoxic compounds. Here, we characterized the consequences of DON co-exposure with acrylamide in a normal intestinal cellular model.

2. Materials and methods

2.1. Cells culture and treatments

IEC-6 cells (ATCC CRL-1592) were cultured in Dulbecco's Modified Eagle Medium (DMEM, Gibco, Life Technologies) supplemented with 10 % fetal bovine serum (FBS, Gibco), 1 % antibiotics (penicillin-streptomycin) and 0.1 U/mL insulin human solution (Sigma-Aldrich). HCT116 (ATCC CCL-247) were cultured in McCoy's 5a Medium Modified (Gibco, Life Technologies) supplemented with 10 % fetal bovine serum (FBS, Gibco). Cells were grown at 37 °C in a humidified atmosphere containing 5 % CO_2 and subcultured every 2–3 days.

DON (D0156, prepared as a 5 mM solution in water; CAS no. 51481-10-8), acrylamide (A4058, 40 % solution in water; CAS no. 79-06-1) etoposide (E1383, prepared as a 50 mM solution in DMSO; CAS no. 33419-42-0) and anisomycin (A9789, prepared as a 75 mM solution in DMSO; CAS no. 22862-76-6) were purchased from Sigma-Aldrich. Deepoxy-deoxynivalenol (DOM-1, 34135, prepared as a 5 mM solution in DMSO; CAS no. 88054-24-4) was purchased from Sigma-Aldrich and prepared as previously described (Willoquet et al., 2024). The pan-caspase inhibitor *Z*-VAD(OMe)-FMK (Z-VAD, T6013, prepared as a 50 mM solution in DMSO; Cas No. 187389-52-2) were purchased from TargetMol. Etoposide, anisomycin and DOM-1 were used at a final concentration of 3 μM, 100 nM and 5 μM, respectively. Z-VAD was added 1 h before DON and/or acrylamide and when cells were released in fresh medium, at a final concentration of 10 μM. During assays requiring the use of etoposide, anisomycin, DOM-1 or Z-VAD, control cells were incubated in the presence of a DMSO vehicle.

2.2. Cell viability assay

IEC-6 and HCT116 cells were seeded in triplicate at a density of 20,000 cells per well in 96-well plates. One day after seeding, cells were treated during 4 h and washed with PBS before being incubated in fresh complete culture medium for 20 h. Viability was assessed using the CellTiter-Glo® Luminescent Cell Viability Assay (Promega) according to the manufacturer's instructions.

2.3. RNAseq gene expression studies

IEC-6 cells were seeded in 60 mm dishes (Falcon reference 353004) at a density of 1.10^6 cells per well. After 24 h of culture, IEC-6 cells were treated with acrylamide 6 mM and DON 3 μM, alone or in mixture, for 4 h. Cells were then collected in Extract-All (Eurobio Scientific) and stored at −80 °C. The samples were processed as described previously (Hasuda et al., 2023). Briefly, the concentrations and purity of RNA were measured with the Nanophotometer^R N60 (Thermo Fisher Scientific). For each of 16 samples, RNAseq libraries were constructed from 1000 ng of total RNA at the GeT-TRiX facility (GénoToul, Génopole Toulouse Midi-Pyrénées) using Illumina® Stranded mRNA Prep kit (Illumina, San Diego, CA, USA) following the manufacturer's instructions. Briefly, mRNAs were captures, then fragmented, converted to double-stranded cDNAs and sequencing adaptors were ligated. Libraries were amplified with ten cycles of PCR. The yield and the quality of the libraries were assessed using D1000 ScreenTapes on TapeStation 4200 (Agilent Technologies, Santa Clara). The libraries were then pooled to equimolar concentrations and transferred to INRAE PGTB facility for sequencing. The library pool was loaded into one flowcell on Illumina Nextseq 2000 using a 2 × 50 bp paired-end sequencing mode with P3 Reagent kit.

Bioinformatics treatments of sequencing data were performed by the GeT-TRiX facility (GenoToul, Génopole Toulouse Midi-Pyrénées) using the computing resources of genotoul bioinformatics platform Toulouse

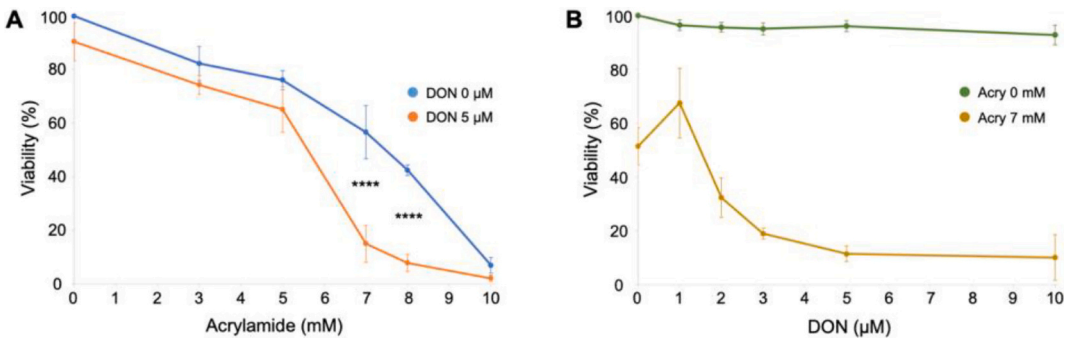

Fig. 1. Cytotoxic interaction between DON and acrylamide. (A, B). IEC-6 cells were exposed to DON and/or acrylamide (Acry) for 4 h followed by 20 h of release in fresh medium before assessing cell viability. IEC-6 cells were treated with increasing concentrations of acrylamide in presence or in absence of DON 5 µM (A) or with increasing concentrations of DON in presence or in absence of acrylamide 7 mM (B). Data are expressed as the mean ± SD of 3 independent experiments. Statistical differences were calculated by two-way ANOVA followed by Sidak's multiple comparison test between conditions with or without DON. (****$p < 0.0001$).

Midi-Pyrenees (Bioinfo Genotoul). The analysis pipeline was executed with Nextflow v22.12.0-edge (Di Tommaso et al., 2017) and processed using nf-core/rnaseq v3.12.0 (https://doi.org/10.5281/zenodo.7998767) of the nf-core collection of workflows (Ewels et al., 2020). Reads were aligned to Rat genome reference mRatBN7.2 (build GCA_015227675.2).

2.4. Immunofluorescence analysis

IEC-6 and HCT116 cells were seeded at a density of 20,000 cells per well in 96-well plates. One day after seeding, cells were treated during 4 h. The immunofluorescence assay was performed as previously described (Pons et al., 2021). Briefly, cells in PBS were fixed with 4 % paraformaldehyde, permeabilized with 0.5 % Triton X-100, and blocked with 3 % BSA and 0.05 % IGEPAL. Cells were stained with a primary antibody directed against γH2AX (Merck/Millipore (05-636-1) or Cell Signaling (20E3)) for 2 h at room temperature in blocking solution, and washed three times with PBS 0.05 % IGEPAL before incubation with secondary antibody (Alexa Fluor 546 Goat anti-mouse (A11030) or anti-rabbit (A11035)) for 1 h at room temperature. DNA was stained with 4.6-diamino-2-phenyl indole (DAPI) at 100 nM. Cells were analyzed using an ImageXpress Micro Confocal High-Content Imaging System (MolecularDevices) with a 20× objective. The level of the nuclear γH2AX signal was quantified in at least 5.000 cells per sample.

2.5. Comet assay

The comet assay was performed under alkaline conditions using a Comet SCGE assay kit (Enzo Life Sciences, Villeurbanne, France) according to the manufacturer's instructions. IEC-6 cells were seeded at a density of 70,000 cells per well in 24-well plates. After one day, cells were treated during 4 h and collected by trypsinization. 10,000 cells embedded in low-melting agarose were spread in each sample area of the comet slide. Electrophoresis was performed in alkaline solution (0.3 N NaOH, 1 mM EDTA) at 4 °C for 15 min at 35 V in a large electrophoresis tank (35 cm between electrodes). After staining with CYGREEN® Nucleic Acid Dye, slides were observed at 20× magnification using a Nikon 50i fluorescence microscope equipped with a Luca S camera. At least 40 cells were analyzed per sample using OpenComet software.

2.6. Cell cycle analyzes by flow cytometry

Cells were seeded at a density of 70,000 cells per well in 24-well plates. After one day, cells were treated during 4 h and washed with PBS before being incubated in fresh complete culture medium for 20 h. Cells were collected by trypsinization and fixed with 4 % paraformaldehyde for 15 min at room temperature in PBS. Cells were permeabilized with 0.5 % Triton X-100 for 15 min followed by staining with DAPI at 1 µg/mL for 15 min at room temperature. Samples were processed using flow-cytometry (MACSQuant, Miltenyi Biotec). At least 10,000 events were analyzed per sample using FlowLogic software (Miltenyi Biotec).

2.7. Apoptosis assay analyzes by flow cytometry

Cells were seeded at a density of 100,000 cells per well in 24-well plates. After one day, cells were treated during 4 h and collected by trypsinization. Early apoptotic and dead cells were scored using the Annexin V-Elab Fluor® 647/DAPI Apoptosis Kit according to the manufacturer's instructions. Samples were processed using flow cytometry (MACSQuant, Miltenyi Biotec). At least 30,000 events were analyzed per sample using FlowLogic software (Miltenyi Biotec).

2.8. Chromosomal aberration assay

Cells were seeded at a density of 1,500,000 cells in 75 cm^2 cell culture flasks. After one day, cells were treated during 4 h and washed with PBS before being incubated in fresh complete culture medium for 20 h. KaryoMAX colcemid solution (Fisher Scientific, Life Technologie) was added for 30 min to block cells in metaphase. Mitotic cells were collected by shake-off and resuspended in a hypotonic solution with 75 mM KCl and incubated for 10 min at 37 °C. Then, cells were fixed in an ethanol/acetic acid solution (3:1) and dropped on slides to spread the chromosomes. VECTASHIELD mounting medium containing DAPI (Vector Laboratories) was added and metaphases were observed at 60 × magnification with a Nikon 50i fluorescence microscope equipped with a Luca S camera.

2.9. Statistics analysis

Biostatistical analyzes of RNA-seq data were performed under R v4.2.2 (R Core Team, 2022), edgeR package (Robinson et al., 2010) and Bioconductor packages (Amezquita et al., 2020). Briefly, raw count table was filtered to eliminate undetected genes using filterByExpr function with min.count = 10. Normalization factors were calculated using TMM method. Then the common, trended and tagwise negative binomial dispersions were estimated with the robust mode of estimateDisp function. A negative binomial generalized log-linear model was fitted to count data with the quasi-likelihood (QL) methods using glmQLFit function to moderate the genewise QL dispersion (McCarthy et al., 2012). Pair-wise comparisons between biological conditions were extracted using specific contrasts with glmQLFtest function to identify differential expression. A correction for multiple testing was applied using Benjamini-Hochberg procedure to control the False Discovery Rate (FDR). Probes with FDR ≤ 0.05 were considered to be differentially

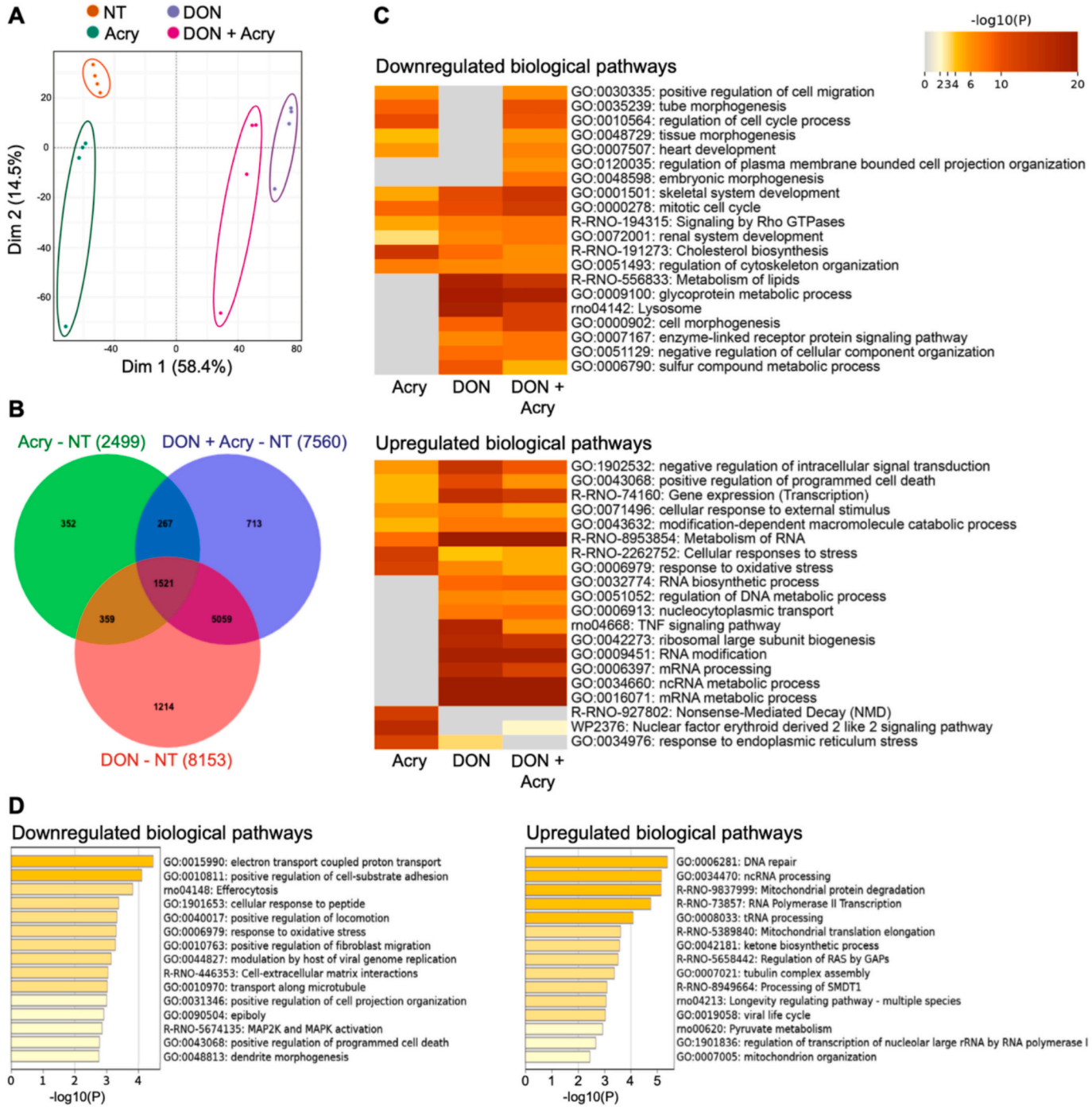

Fig. 2. Transcriptional response to DON and acrylamide co-exposure. (A) Principal component analysis (PCA) score plots of the whole transcriptomic dataset (normalized log2 counts per million) of IEC-6 cells exposed to DON, acrylamide (Acry), DON and acrylamide (DON + Acry) or left non-treated (NT). (B) Venn diagram representing the number of genes significantly modulated (FDR < 5 %) by DON, acrylamide (Acry) or both (DON + Acry). (C) Heatmaps of pathway enrichment analysis based on the most significantly modulated genes (FDR < 0.1 %) after exposure to DON, acrylamide (Acry) or both (DON + Acry). The top 20 down- or upregulated biological pathways are represented with a color scale for statistical significance. (D) Bar graph of the gene clusters enriched based on the 713 genes specifically modulated after co-exposure to DON and acrylamide as shown in (B). The top 15 down- or upregulated biological pathways are represented.

expressed between conditions.

Gene ontology analyzes were performed with the Metascape tool (https://metascape.org/) applying standard parameters (Zhou et al., 2019). All other statistical analyzes were assessed using Prism 10 software (GraphPad). For the chromosomal aberration assay, Chi^2 Pearson and Fisher's exact tests were performed. For the other tests, one-way or two-way ANOVA analyzes of variance followed by *post hoc* tests (Sidak or Tukey when appropriate) were performed. The results are expressed as the mean with Standard deviation (SD).

3. Results

3.1. DON and acrylamide co-exposure increases cytotoxicity

To determine whether DON aggravates acrylamide-induced cytotoxicity, rat intestinal epithelial cells (IEC-6) were exposed to increasing

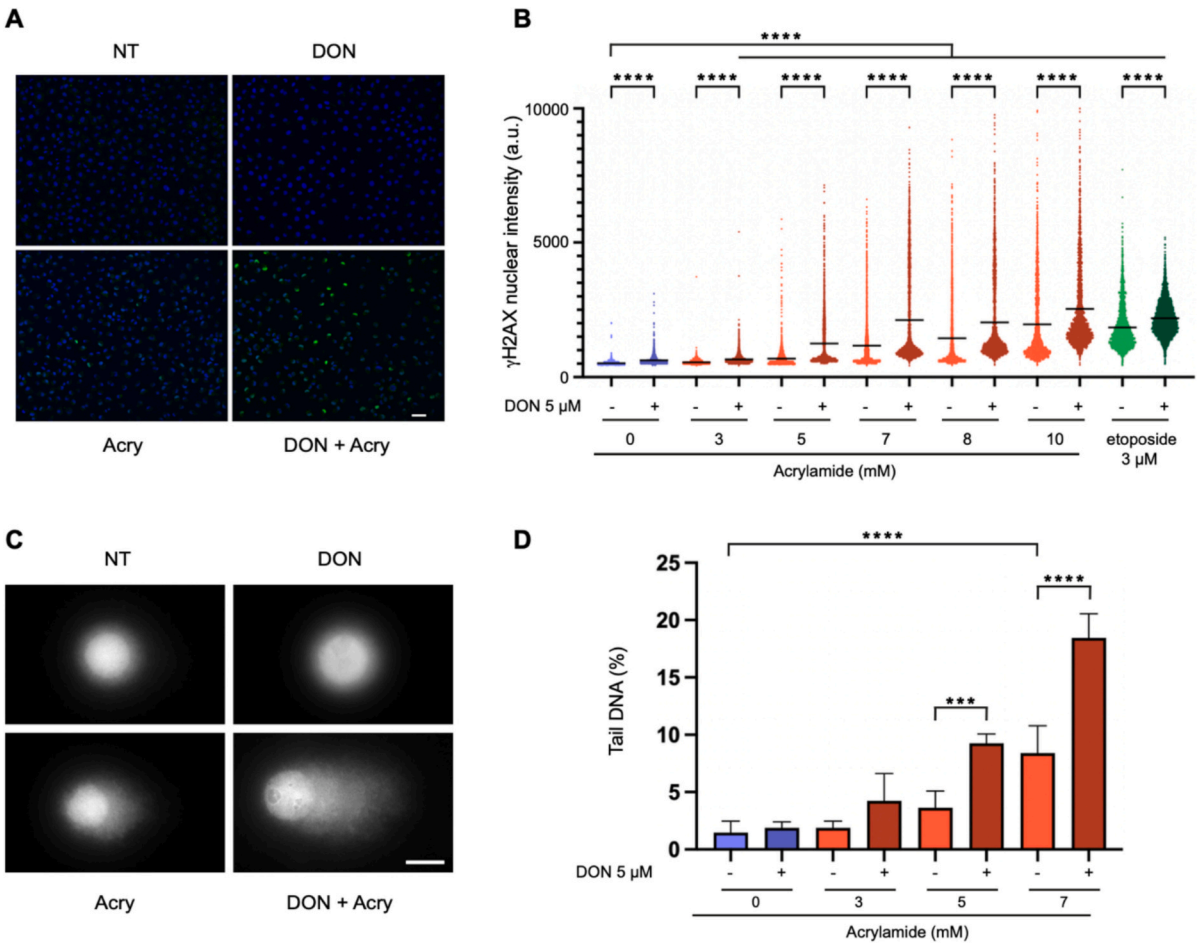

Fig. 3. DON exacerbates acrylamide-induced DNA damage. IEC-6 cells were exposed for 4 h to increasing concentrations of acrylamide (Acry) in presence or in absence of DON 5 μM before assessing genotoxicity. (A). Representative images of γH2AX immunostaining (green) in IEC-6 cells exposed to DON and/or acrylamide 7 mM. DNA was stained with DAPI (blue). NT represents non-treated cells. Scale bar = 20 μm. (B). Quantification of γH2AX signal from (A), represented as the mean fluorescence intensity per nucleus in arbitrary units (a.u.) of one representative among 3 independent experiments. Black lines indicate mean. Statistical differences were calculated by one-way ANOVA followed by Tukey's multiple comparison test between the indicated conditions (****$p < 0.0001$). (C). Representative images of non-treated cells (NT) or cells treated with DON and/or acrylamide 7 mM and evaluated with alkaline comet assay. Scale bar = 20 μm. (D). Quantification of tail DNA percentage from (C). Data are expressed as the mean ± SD of at least 3 independent experiments. Statistical differences were calculated by two-way ANOVA followed by Tukey's multiple comparison test between the indicated conditions (***$p < 0.001$; ****$p < 0.0001$).

concentrations of acrylamide, with or without 5 μM of DON (Fig. 1A). Conversely, a dose-response to DON cytotoxic effects was performed in presence or in absence of 7 mM of acrylamide (Fig. 1B). A dose-dependent cytotoxicity was observed with acrylamide (Fig. 1A), whereas DON alone induced no obvious effect on cell viability up to 10 μM (Fig. 1B). Remarkably, cells co-exposed to acrylamide and DON showed a significant increase of cytotoxicity compared to acrylamide alone. These results pinpoint the cytotoxic interaction between DON and acrylamide.

3.2. Transcriptional response to DON and acrylamide co-exposure supports a genotoxic interaction

Then, a genome wide transcriptomic analysis was performed on IEC-6 cells exposed to acrylamide, DON or both, in comparison to untreated control cells. Principal component analysis revealed that while each group can be separated, the overall variability is primarily due to DON exposure (Fig. 2A). Venn diagrams confirmed that DON modulated the expression of more genes compared to acrylamide or to DON with acrylamide (Fig. 2B). Moreover, 75.2 % and 86.6 % of genes differentially expressed by acrylamide or by DON and acrylamide co-exposure, respectively, are also modulated by DON alone. Thus, under our conditions, DON exerted a major effect on gene regulation, covering the larger part of the transcriptional response to acrylamide or to both compounds.

Then, we compared the most significantly down- and upregulated biological pathways after exposure to DON, acrylamide, or both. The vast majority (92 %) of the pathways modulated by co-exposure were also regulated by DON or acrylamide alone (Fig. 2C and Sup Figs. 1 and 2). Common downregulated pathways include cell cycle processes while upregulated pathways include programmed cell death and the cellular response to different stress including oxidative stress. Interestingly, the acrylamide-mediated upregulation of pathways associated to the unfolded protein response or to NRF2, a transcription factor driving the cellular defense against toxic and oxidative insults, were decreased or lost in presence of DON, suggesting a specific responses to co-exposure (Fig. 2C, Sup Fig. 2).

In light of this, we next examined the 713 RNA only modulated under the co-exposure condition (Fig. 2b). Strikingly, the most upregulated biological pathway concerns DNA repair (Fig. 2D), indicating a genotoxic interaction. Conversely, responses to peptide or oxidative stress and the related mitogen-activated protein kinase (MAPK)/MAP2K activation were decreased, in contrast to their acrylamide-mediated upregulation (Fig. 2C and Sup Fig. 1). Taken together, our data demonstrate that co-exposure to DON and acrylamide globally recapitulates the transcriptional response to each compound individually, the most

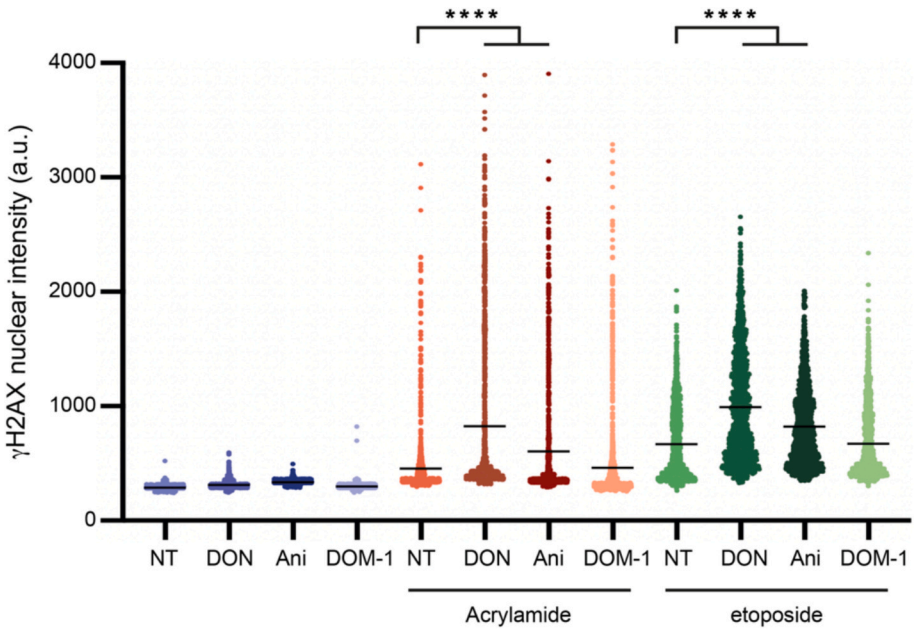

Fig. 4. Anisomycin but not DOM-1 exacerbates acrylamide-induced DNA damage. IEC-6 cells were exposed for 4 h to DON 5 μM, anisomycin (Ani) 100 nM, DOM-1 5 μM, or left untreated (NT), in presence or in absence of acrylamide 7 mM or etoposide 3 μM. Quantification of γH2AX signal is represented as the mean fluorescence intensity per nucleus in arbitrary units (a.u.) of one representative among 3 independent experiments. Black lines indicate mean. Statistical differences were calculated by one-way ANOVA followed by Tukey's multiple comparison test between the indicated conditions (****$p < 0.0001$).

important part being attributable to DON. However, few processes are specifically regulated by DON and acrylamide interaction, as enhanced DNA repair or decreased response to oxidative stress. This supports a genotoxic interaction and suggests that co-exposure may perturb the normal response to DON or acrylamide.

3.3. DON exacerbates the genotoxicity of acrylamide

We next evaluated the level of acrylamide-induced DNA damage in presence of DON. First, the induction of the DNA damage biomarker γH2AX was measured by immunofluorescence analyzes (Fig. 3A). Signal quantification shows that acrylamide causes a dose-dependent increase of the nuclear γH2AX induction after 4 h (Fig. 3B). IEC-6 cells exposed to DON 5 μM exhibited a slight increase in γH2AX compared to untreated cells. However, when added to acrylamide or to the DNA damaging agent etoposide used as positive control, DON induces a significant enhancement of the γH2AX level. From the 5 mM acrylamide exposure condition, this increase is stronger than the cumulative effect of each individual compound, suggesting an interaction that could be higher than an additive effect. To strengthen this result, an alkaline comet assay was performed under similar exposure conditions. While DON alone does not significantly increase tail DNA compared to control cells, acrylamide induced a dose-dependent DNA fragmentation (Fig. 3C and D). Similar to γH2AX immunofluorescence analyzes, the presence of DON enhances the acrylamide-induced DNA damage, as revealed by a greater amount of fragmented DNA compared to acrylamide alone.

Finally, to demonstrate that the genotoxic interaction between DON and acrylamide is not specific to rat cells, γH2AX immunofluorescence assays were conducted on the human HCT116 colonic cancer cell line. Using the same experimental design as for IEC-6 cells, we show that while HCT116 cells suffer less viability loss and therefore no obvious cytotoxic interaction (Sup Fig. 3A), DON still exacerbates DNA damage induced by acrylamide in human cells (Sup Fig. 3B). Taken together, these data demonstrate that the genotoxic activity of acrylamide is exacerbated by DON in intestinal cells.

3.4. DNA damage exacerbation by DON involves ribosome inhibition

To examine whether the DON-induced exacerbation of acrylamide genotoxicity is mediated by ribosome inhibition, the ribotoxin anisomycin and DOM-1, a non-ribotoxic modified form of DON, were used in combination with acrylamide. In a similar way to DON, adding anisomycin to acrylamide or etoposide increases γH2AX signal, whereas DOM-1 has no effect (Fig. 4). These results indicate that DON ribotoxicity is important for the genotoxic interaction with acrylamide.

3.5. DNA damage exacerbation by DON does not rely on apoptosis

In order to rule out the hypothesis that DON-mediated DNA damage exacerbation could be related to an apoptotic process, cells were scored by flow cytometry after staining with Annexin V in combination with DAPI to exclude dead cells. After 4 h, acrylamide but not DON promotes early apoptosis (Annexin $V^+/DAPI^-$) in a dose-dependent manner (Fig. 5A). However, DON significantly limits the proportion of acrylamide-induced early apoptosis. Instead, more $DAPI^+$ cells accumulate in presence of DON and acrylamide 10 mM, which could derive from different type of cell death. Altogether, this data indicates that DON does not increase the proportion of early apoptosis after 4 h of acrylamide. Then, the pan-caspase inhibitor *Z*-VAD-OMe-FMK (ZVAD) was added to prevent apoptosis (Sup Fig. 4A), resulting in a non-significant rescue of acrylamide-mediated loss of cell viability (Sup Fig. 4B). In addition, the presence of ZVAD did not impact the level of DNA damage after exposure to acrylamide with or without DON, evaluated by γH2AX immunofluorescence (Fig. 5B) or comet assay (Fig. 5C). To conclude, these data demonstrate that the genotoxic interaction between DON and acrylamide does not result from apoptotic-related DNA fragmentation.

3.6. DON enhances the acrylamide-induced cell cycle arrest

To investigate the consequences of the DON-induced exacerbation of acrylamide genotoxic activity, we first monitored cell cycle checkpoints by flow cytometry. When IEC-6 cells were exposed to acrylamide or

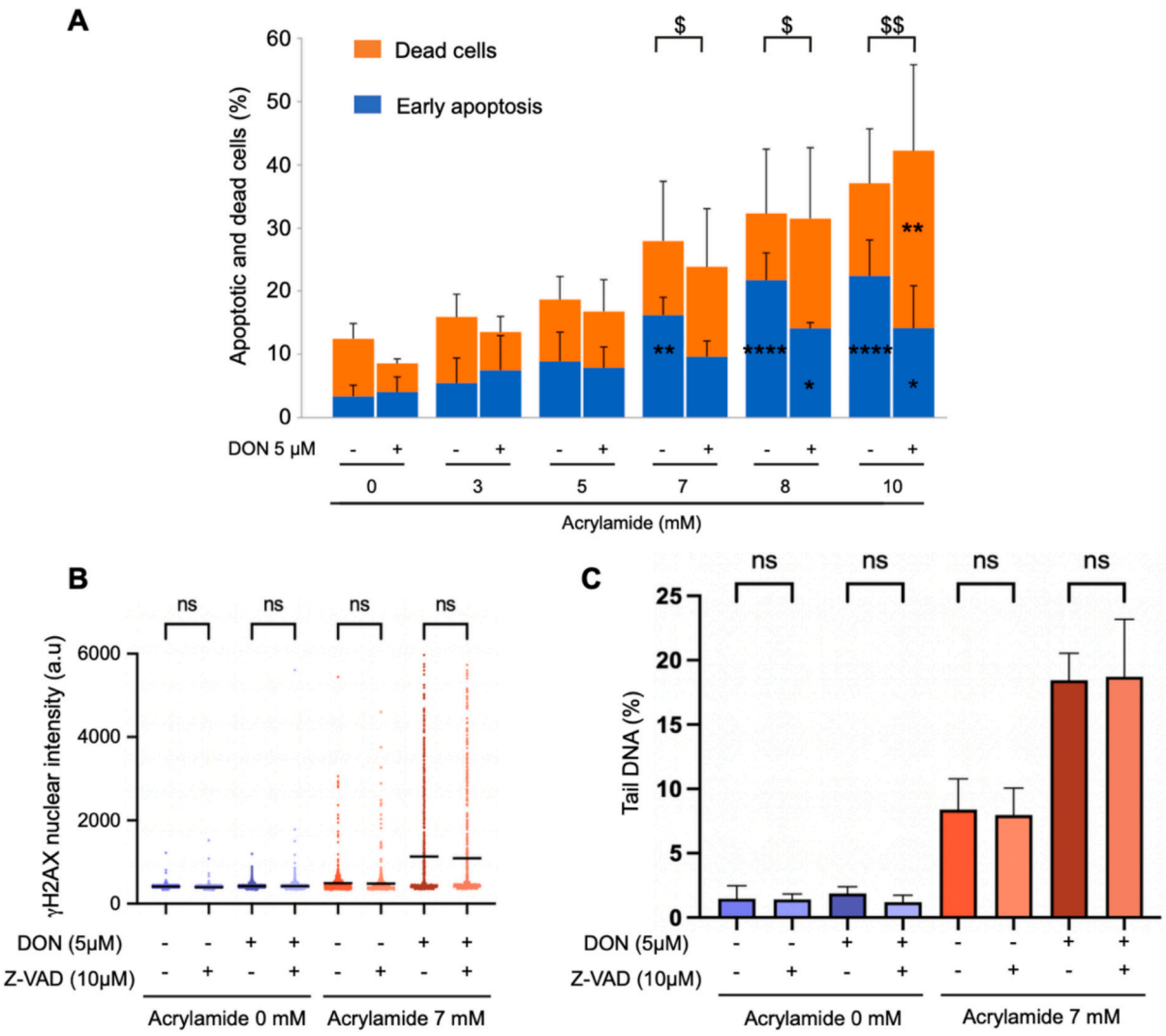

Fig. 5. DON-mediated genotoxicity exacerbation is not related to apoptosis. IEC-6 cells were exposed or not for 1 h to *Z*-VAD 10 µM followed by 4 h to DON 5 µM and/or acrylamide at the indicated concentrations, before assessing apoptosis (A) or genotoxicity (B and C). (A). Cells were exposed to increasing concentrations of acrylamide (Acry) in presence or in absence of DON 5 µM and analyzed by flow-cytometry. The proportion of early apoptotic (Annexin $V^+/DAPI^-$) or dead cells ($DAPI^+$) was measured. Data are expressed as the mean + SD of one representative among 3 independent experiments. Statistical differences were calculated by two-way ANOVA followed by Tukey's multiple comparison test, by comparing to the non-treated cells (indicated by asterisks) or between the conditions with or without DON (indicated by dollars) (* or $ $p < 0.05$; ** or $$ $p < 0.01$; **** $p < 0.0001$). (B). Quantification of γH2AX signal in cells exposed to DON and/or acrylamide with or without Z-VAD, represented as the mean fluorescence intensity per nucleus in arbitrary units (a.u.) of 3 independent experiments. Black lines indicate mean. Statistical differences were calculated by one-way ANOVA followed by Tukey's multiple comparison test between condition with or without Z-VAD. (C). Quantification of tail DNA percentage in cells exposed to DON and/or acrylamide with or without Z-VAD. Data are expressed as the mean ± SD of at least 3 independent experiments. Statistical differences were calculated by two-way ANOVA followed by Sidak's multiple comparison test between conditions with or without Z-VAD (ns: non-significant).

DON alone, no alteration of the cell cycle profile could be observed (Fig. 6), in comparison with control cells. However, the co-exposure condition induces a dose-dependent increase of the proportion of G2/M cells. These data suggest that DON worsen the cell cycle defects caused by acrylamide.

3.7. DON aggravates chromosome instability induced by acrylamide

Finally, chromosomal aberration assays were performed to assess the effect of DON genotoxic interaction with acrylamide on chromosomal stability. Metaphase spreads of IEC-6 cells treated with acrylamide and/or DON were prepared (Fig. 7A), and the percentage of abnormal metaphases was determined (Fig. 7B). Acrylamide but not DON increased the proportion of abnormal metaphases compared to untreated cells. Strikingly, the rate of abnormal metaphases was significantly higher after co-exposure to DON and acrylamide compared to acrylamide alone. Thus, DON enhances the chromosome structural defects caused by acrylamide. To further detail how acrylamide affects chromosomal stability in presence of DON, the different types of aberrations were counted (Fig. 7C). In untreated cells, 89 % of aberrations represent chromosome breaks and 11 % rearrangements, which is not significantly different in DON-exposed cells. Yet, 3.35 % of the DON-induced aberrations were scored as multiple aberrations, representing metaphases with too many aberrations to be properly quantified (Clare, 2012) that were not observed in control conditions. In cells exposed to acrylamide alone or in combination with DON, the number of aberrations per metaphase increased by 2.5- and 3.5-fold compared to control, respectively, but only cells treated with DON exhibited multiple aberrations. Therefore, our data indicate that acrylamide enhances the different types of aberrations naturally occurring in IEC-6 cells, and

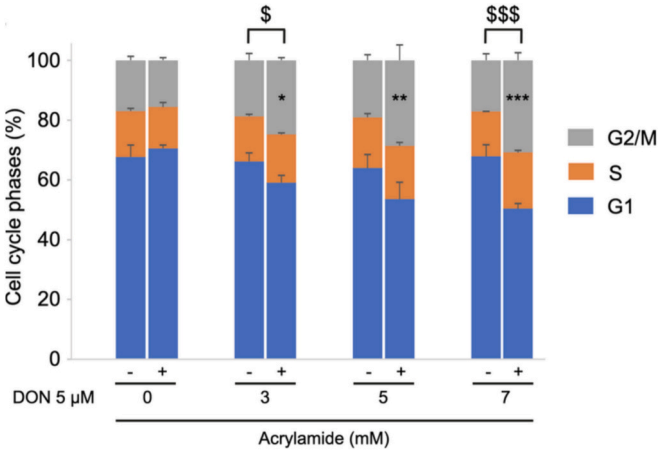

Fig. 6. Cell cycle defects after co-exposure to DON and acrylamide. IEC-6 cells were exposed to DON 5 µM and/or acrylamide at the indicated concentrations for 4 h followed by 20 h of release in fresh medium before cell cycle analysis by flow-cytometry. Cell cycle indexes are shown. Data represent the mean + SD of 3 independent experiments. Statistical differences were only calculated for G2/M cells by two-way ANOVA followed by Tukey's multiple comparison test, by comparing to the non-treated cells (indicated by asterisks) or between the conditions with or without DON (indicated by dollars) (* or $ $p < 0.05$, ** $p < 0.01$; *** or $$$ $p < 0.001$).

DON aggravates this chromosome instability.

4. Discussion

Assessing the combined toxicity of food contaminants is a tremendous challenge that currently remains under-evaluated. Recent studies have shown that DON exacerbates the genotoxicity of a fungicide and a bacterial toxin associated with colorectal cancer (Garofalo et al., 2023; Payros et al., 2017), supporting for potential harmful interaction with other genotoxic food contaminants. In this study, we demonstrate that DON aggravates the genotoxic potential of acrylamide, enhancing DNA damage and genetic instability.

First, transcriptomic analyzes suggest that the toxic interaction between DON and acrylamide mainly reflects an additive effect, predominantly influenced by DON. DON increases RNA metabolism or inflammatory response and decreases lipid metabolism, as previously observed (Luo et al., 2021; Ma et al., 2024; Zhang et al., 2023). Besides, alone or in mixture, DON and acrylamide reduce the expression of genes involved in cell division and enhance genes involved in programmed cell death, two well-known cellular consequences of DNA damage. Of note, DNA repair process is specifically upregulated in co-exposed cells, strengthening the hypothesis of genotoxicity exacerbation by DON.

To investigate the effect of DON on acrylamide-induced genotoxicity, we measured nuclear γH2AX, a well-established marker of DNA damage (Rogakou et al., 1998). The γH2AX level was remarkably higher in co-exposed cells compared to cells exposed to DON or acrylamide individually, corroborating the assumption of a synergistic interaction. This result was strengthened by comet assay that directly assess DNA fragmentation, demonstrating that DON genuinely potentiates acrylamide-induced genotoxicity rather than only perturbing γH2AX-related signaling pathways.

While considered as not genotoxic, we found that DON alone slightly but significantly increases γH2AX level in exposed cells. In the same way, a minor part of metaphases exhibited multiple chromosome aberrations after DON treatment. Previous *in vitro* studies reported contradictory results regarding DON capacity to induce DNA damage

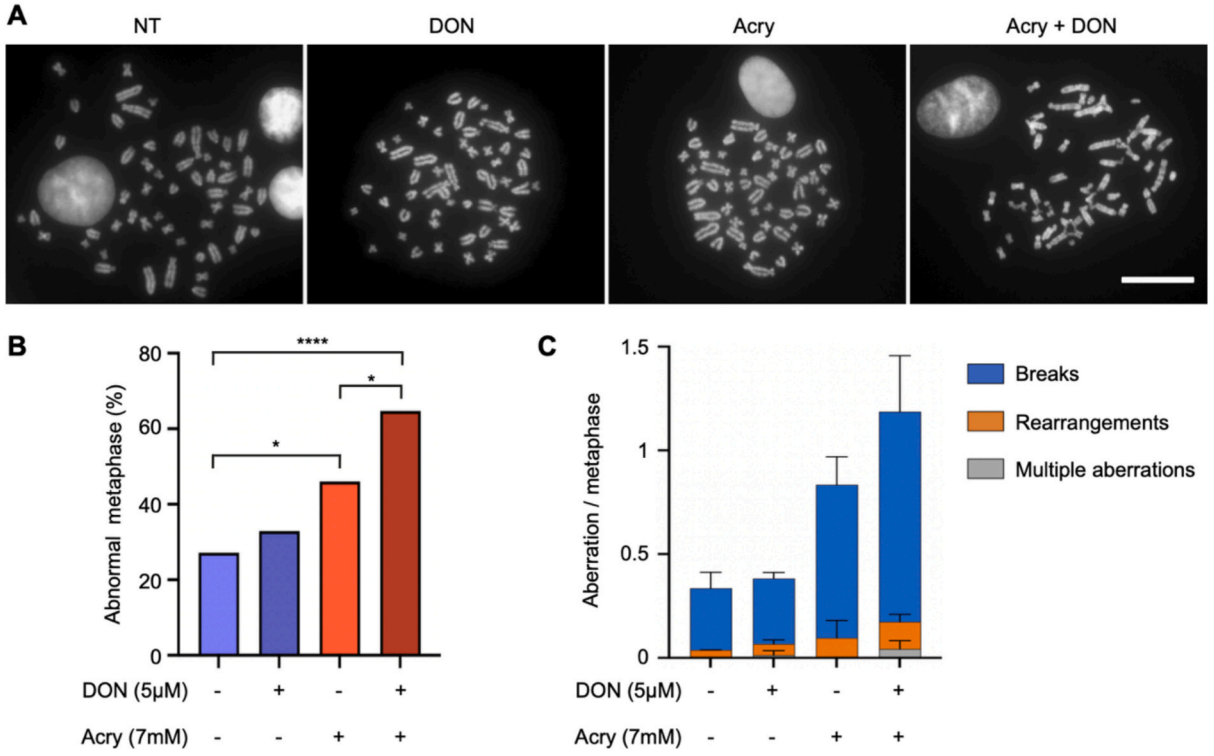

Fig. 7. DON exacerbates acrylamide-induced chromosomal instability. IEC-6 cells were exposed to DON 5 µM and/or acrylamide (Acry) 7 mM for 4 h followed by 20 h of release in fresh medium before preforming metaphase spreads. (A). Representative images of metaphase spreads of cells exposed to DON and/or acrylamide or left non-treated cells (NT). Scale bar = 20 µm. (B). Quantification of metaphases from (A) with at least one chromosomal aberration. At least 60 metaphases from 3 independent experiments were analyzed. Statistical differences were calculated by Chi^2 test between the indicated conditions (*$p < 0.05$; ****$p < 0.0001$). (C). Quantification of aberrations per metaphase from (A). The different types of aberrations are classified as breaks, rearrangements or multiple aberrations (see the text for more details).

(Garofalo et al., 2022; Garofalo et al., 2023; Kopp et al., 2018; Takakura et al., 2014; Zhang et al., 2009), which may be explained by the use of different cell lines, exposure conditions or method sensitivity. Further studies will be necessary to clarify this point.

Our data support that DON aggravates the genotoxic activity of acrylamide. However, an indirect effect resulting from enhanced apoptosis could not be excluded, given that DON and acrylamide are two apoptotic inducers (Pestka, 2008; Song et al., 2021). Indeed, apoptotic processes implicate massive genomic DNA fragmentation after activation of apoptotic nucleases (Basnakian & Moore, 2021), resulting in high γH2AX level (Rogakou et al., 2000) and giving rise to false positive during comet assay (Choucroun et al., 2001). Our results revealed that after a 4 h co-exposure, where the genotoxicity exacerbation is observed, DON does not increase the proportion of acrylamide-induced early apoptotic cells. In addition, the apoptosis inhibitor ZVAD does not alleviate the amount of DNA damage (Fig. 5B and C). Thus, in cells exposed to acrylamide, DNA damage exacerbation by DON does not result from apoptotic processes.

Cells under genotoxic stress activate cell cycle checkpoints to avoid entering mitosis in presence of DNA lesions (Waterman et al., 2020). It has previously been shown that acrylamide induces cell cycle arrest at G2/M (Wang et al., 2022). After an acrylamide treatment followed by a 20 h release in fresh medium, no obvious defect in cell cycle was observed (Fig. 6), suggesting that the release time allowed sufficient DNA repair to inactivate checkpoints and restart a normal cell cycle. In contrast, cells co-exposed to DON and acrylamide present a G2/M block, indicative of a more pronounced genotoxic stress. This suggests that the amount of DNA damage in presence of DON exceeded the DNA repair capacity necessary to restart cell cycle. Understanding how DON alters the equilibrium between DNA damage and DNA repair will permit to better characterize the toxic interaction between DON and genotoxic compounds.

Chromosomal aberrations are characteristics of cancerous cells, observed in over 90 % of solid and blood cancers (Hosea et al., 2024). Acrylamide is known to induce chromosome structural alterations *in vivo* (Algarni, 2018; Shiraishi, 1978). Here, we found that DON increases the proportion of acrylamide-induced chromosome damage, either breaks or rearrangements. Given that acrylamide is considered as a probable human carcinogen (International Agency for Research on Cancer, 1994) whereas DON is not (Claeys et al., 2020), our data suggest that DON could foster acrylamide carcinogenic properties. However, this has to be confirmed by *in vivo* experimentation.

Another recent study has analyzed the combined effect of DON and acrylamide in the hepatic HepaRG cell line, showing that the mixture cytotoxicity is specifically attributable to DON with only a negligible effect of acrylamide (Beisl et al., 2024). However, in contrast to our study conducted on proliferative intestinal IEC-6 cells, *Beisl* et al. used differentiated cells to be metabolically active, but at the expense of proliferative capacity. As this can greatly influence cytotoxicity, the results obtained with IEC-6 and HepaRG cells cannot be directly compared.

As previously demonstrated with other DNA damaging agents, exacerbation by DON of acrylamide genotoxicity relies on ribosome inhibition (Garofalo et al., 2022). Nevertheless transcriptomic analyzes conducted in this study may also provide some hypotheses to better understand the link between DON and acrylamide toxic interaction and enhanced genotoxicity. Acrylamide and to a lesser extend DON upregulate pathways involved in response to cellular stresses, including oxidative stress. Acrylamide toxicity is closely linked to oxidative stress and induces a related transcriptional response in rodent liver (Mei et al., 2008; Yousef & El-Demerdash, 2006). Similarly, the intestine is also vulnerable to the harmful effects of acrylamide-mediated oxidative stress (Palus, 2024). As the intestinal toxicity of DON is at least partly attributable to reactive oxygen species (ROS) overproduction (Wang et al., 2021), which has already been observed in IEC-6 cells (Del Regno et al., 2015), one could speculate that the toxic interaction between DON and acrylamide could involve oxidative stress accumulation. Interestingly, in presence of DON, the acrylamide-dependent upregulation of oxidative stress response, including the NRF2 pathway, is perturbed. This suggests that DON may diminish the antioxidant capacity of acrylamide-treated cells, aggravating acrylamide genotoxicity. Further analyzes are required to address this point.

It is assumed that as high as 35 % of environmental factors that contribute to the onset of cancer are associated with diet (Baena Ruiz & Salinas Hernández, 2014). Compared to other risk factors, food represents a readily modifiable element for improving cancer prevention through dietary changes (Britten & Tosi, 2024). Considering the high prevalence of DON in human food (De Santis et al., 2019) and the recent findings regarding its ability to exacerbate DNA damage induced by various compounds (Garofalo et al., 2022; Garofalo et al., 2023a; Payros et al., 2017), deciphering DON pro-carcinogenic interactions with genotoxic food contaminants is of crucial concern. In this study, we bring evidence supporting that DON may aggravate the adverse effects associated with consumption of acrylamide, a probable carcinogen already known to represent a public health risk according to EFSA (EFSA CONTAM Panel, 2015). Our findings imply that DON and acrylamide tolerable daily intake that have been calculated based on their individual toxicity should be refined due to their genotoxic interaction.

CRediT authorship contribution statement

Chloé Huertas: Writing – review & editing, Writing – original draft, Methodology, Investigation, Formal analysis, Conceptualization. **Aboubacar B. Coulibaly:** Methodology, Investigation. **Delphine Payros:** Writing – review & editing, Writing – original draft, Funding acquisition, Conceptualization. **Marie Penary:** Methodology, Investigation. **Sylvie Puel:** Methodology, Investigation. **Claire Naylies:** Methodology, Investigation. **Gaëlle Payros:** Conceptualization. **Yannick Lippi:** Writing – review & editing, Formal analysis, Data curation, Conceptualization. **Isabelle P. Oswald:** Writing – review & editing, Funding acquisition, Conceptualization. **Gladys Mirey:** Writing – review & editing, Conceptualization. **Julien Vignard:** Writing – review & editing, Writing – original draft, Supervision, Project administration, Methodology, Investigation, Funding acquisition, Formal analysis, Conceptualization.

Declaration of competing interest

The authors declare the following financial interests/personal relationships which may be considered as potential competing interests: Julien Vignard reports financial support was provided by French National Research Agency. Isabelle P. Oswald reports financial support was provided by French National Research Agency. Delphine Payros reports financial support was provided by Olga Triballat Institute. Delphine Payros reports financial support was provided by Roquette Fundation. If there are other authors, they declare that they have no known competing financial interests or personal relationships that could have appeared to influence the work reported in this paper.

Acknowledgments

The authors would like to express their gratitude to Dr. Marc Audebert for giving access to the High-Content Imaging System, and Dr. Frédéric Catez for valuable suggestions on this study. We thank Dr. Sandrine Ellejo-Simatos for comments on statistical analyzes, and Zoé Compagnie for the sequencing of libraries at INRAE PGTB sequencing facility (doi:10.15454/1.5572396583599417E12). We are grateful to the genotoul bioinformatics platform Toulouse Midi-Pyrénées (Bioinfo Genotoul) for providing computing resource. This work was supported by grants from the French Olga Triballat Institute and the French Roquette Foundation, and from the French Agence Nationale de la Recherche (Genofood ANR-19-34CE and GenoMyc ANR-22-34CE).

Appendix A. Supplementary data

Supplementary data to this article can be found online at https://doi.org/10.1016/j.foodres.2025.116633.

Data availability

RNAseq data and experimental details are available in NCBI's Gene Expression Omnibus and are accessible through GEO Series accession number GSE291848. Data will be made available on request.

References

Alassane-Kpembi, I., Schatzmayr, G., Taranu, I., Marin, D., Puel, O., & Oswald, I. P. (2017). Mycotoxins co-contamination: Methodological aspects and biological relevance of combined toxicity studies. *Critical Reviews in Food Science and Nutrition, 57*, 3489–3507. https://doi.org/10.1080/10408398.2016.1140632

Algarni, A. A. (2018). Genotoxic effects of acrylamide in mouse bone marrow cells. *Caryologia, 71*, 160–165. https://doi.org/10.1080/00087114.2018.1450801

Amezquita, R. A., Lun, A. T. L., Becht, E., Carey, V. J., Carpp, L. N., Geistlinger, L., … Hicks, S. C. (2020). Orchestrating single-cell analysis with bioconductor. *Nature Methods, 17*, 137–145. https://doi.org/10.1038/s41592-019-0654-x

Baena Ruiz, R., & Salinas Hernández, P. (2014). Diet and cancer: Risk factors and epidemiological evidence. *Maturitas, 77*, 202–208. https://doi.org/10.1016/j.maturitas.2013.11.010

Balbo, C., & Woźniak, Ł. (2022). Dietary exposure and risk characterisation of multiple chemical contaminants in rye-wheat bread marketed in Poland. *EFSA Journal, 20*, Article e200911. https://doi.org/10.2903/j.efsa.2022.e200911

Basnakian, A. G., & Moore, C. L. (2021). Apoptotic DNase network: Mutual induction and cooperation among apoptotic endonucleases. *Journal of Cellular and Molecular Medicine, 25*, 6496–6499. https://doi.org/10.1111/jcmm.16665

Beisl, J., Jochum, K., Chen, Y., Varga, E., & Marko, D. (2024). Combinatory effects of acrylamide and Deoxynivalenol on in vitro cell viability and cytochrome P450 enzymes of human HepaRG cells. *Toxins, 16*, 389. https://doi.org/10.3390/toxins16090389

Bogdanova, E., Rozentale, I., Pugajeva, I., Emecheta, E. E., & Bartkevics, V. (2018). Occurrence and risk assessment of mycotoxins, acrylamide, and furan in Latvian beer. *Food Additives & Contaminants: Part B, 11*, 126–137. https://doi.org/10.1080/19393210.2018.1440636

Britten, O., & Tosi, S. (2024). The role of diet in cancer: The potential of shaping public policy and clinical outcomes in the UK. *Genes & Nutrition, 19*, 15. https://doi.org/10.1186/s12263-024-00750-9

Choucroun, P., Gillet, D., Dorange, G., Sawicki, B., & Dewitte, J. D. (2001). Comet assay and early apoptosis. *Mutation Research, Fundamental and Molecular Mechanisms of Mutagenesis, 478*, 89–96. https://doi.org/10.1016/S0027-5107(01)00123-3

Cinar, A., & Onbaşı, E. (2020). Mycotoxins: The hidden danger in foods. *Intechopen*. https://doi.org/10.5772/intechopen.89001

Claeys, L., Romano, C., De Ruyck, K., Wilson, H., Fervers, B., Korenjak, M., … Huybrechts, I. (2020). Mycotoxin exposure and human cancer risk: A systematic review of epidemiological studies. *Comprehensive Reviews in Food Science and Food Safety, 19*, 1449–1464. https://doi.org/10.1111/1541-4337.12567

Clare, G. (2012). The in vitro mammalian chromosome aberration test. In J. M. Parry, & E. M. Parry (Eds.), *Genetic toxicology, methods in molecular biology* (pp. 69–91). New York, New York, NY: Springer. https://doi.org/10.1007/978-1-61779-421-6_5.

De Santis, B., Debegnach, F., Miano, B., Moretti, G., Sonego, E., Chiaretti, A., … Brera, C. (2019). Determination of deoxynivalenol biomarkers in Italian urine samples. *Toxins, 11*, 441. https://doi.org/10.3390/toxins11080441

Del Regno, M., Adesso, S., Popolo, A., Quaroni, A., Autore, G., Severino, L., & Marzocco, S. (2015). Nivalenol induces oxidative stress and increases deoxynivalenol pro-oxidant effect in intestinal epithelial cells. *Toxicology and Applied Pharmacology, 285*, 118–127. https://doi.org/10.1016/j.taap.2015.04.002

Di Tommaso, P., Chatzou, M., Floden, E. W., Barja, P. P., Palumbo, E., & Notredame, C. (2017). Nextflow enables reproducible computational workflows. *Nature Biotechnology, 35*, 316–319. https://doi.org/10.1038/nbt.3820

EFSA CONTAM Panel. (2015). Scientific opinion on acrylamide in food. *EFSA Journal, 13*, 4104. https://doi.org/10.2903/j.efsa.2015.4104

Eskola, M., Kos, G., Elliott, C. T., Hajšlová, J., Mayar, S., & Krska, R. (2020). Worldwide contamination of food-crops with mycotoxins: Validity of the widely cited "FAO estimate" of 25. *Critical Reviews in Food Science and Nutrition, 60*, 2773–2789. https://doi.org/10.1080/10408398.2019.1658570

European Food Safety Authority. (2013). Deoxynivalenol in food and feed: Occurrence and exposure. *EFSA Journal, 11*, 3379. https://doi.org/10.2903/j.efsa.2013.3379

Ewels, P. A., Peltzer, A., Fillinger, S., Patel, H., Alneberg, J., Wilm, A., … Nahnsen, S. (2020). The nf-core framework for community-curated bioinformatics pipelines. *Nature Biotechnology, 38*, 276–278. https://doi.org/10.1038/s41587-020-0439-x

Garofalo, M., Payros, D., Oswald, E., Nougayrède, J.-P., & Oswald, I. P. (2022). The foodborne contaminant deoxynivalenol exacerbates DNA damage caused by a broad spectrum of genotoxic agents. *Science of the Total Environment, 820*, Article 153280. https://doi.org/10.1016/j.scitotenv.2022.153280

Garofalo, M., Payros, D., Penary, M., Oswald, E., Nougayrède, J.-P., & Oswald, I. P. (2023). A novel toxic effect of foodborne trichothecenes: The exacerbation of genotoxicity. *Environmental Pollution, 317*, Article 120625. https://doi.org/10.1016/j.envpol.2022.120625

Garofalo, M., Payros, D., Taieb, F., Oswald, E., Nougayrède, J.-P., & Oswald, I. P. (2025). From ribosome to ribotoxins: Understanding the toxicity of deoxynivalenol and Shiga toxin, two food borne toxins. *Critical Reviews in Food Science and Nutrition, 65* (1), 193–205. https://doi.org/10.1080/10408398.2023.2271101

Guth, S., Baum, M., Cartus, A. T., Diel, P., Engel, K.-H., Engeli, B., Epe, B., Grune, T., Haller, D., Heinz, V., Hellwig, M., Hengstler, J. G., Henle, T., Humpf, H.-U., Jäger, H., Joost, H.-G., Kulling, S. E., Lachenmeier, D. W., Lampen, A., … Eisenbrand, G. (2023). Evaluation of the genotoxic potential of acrylamide: Arguments for the derivation of a tolerable daily intake (TDI value). *Food and Chemical Toxicology, 173*, Article 113632. https://doi.org/10.1016/j.fct.2023.113632

Hasuda, A. L., Person, E., Khoshal, A., Bruel, S., Puel, S., Oswald, I. P., … Pinton, P. (2023). Emerging mycotoxins induce hepatotoxicity in pigs' precision-cut liver slices and HepG2 cells. *Toxicon, 231*, Article 107195. https://doi.org/10.1016/j.toxicon.2023.107195

Hosea, R., Hillary, S., Naqvi, S., Wu, S., & Kasim, V. (2024). The two sides of chromosomal instability: Drivers and brakes in cancer. *Signal Transduction and Targeted Therapy, 9*, 1–30. https://doi.org/10.1038/s41392-024-01767-7

International Agency for Research on Cancer. (1994). Acrylamide. *IARC Monographs on the Evaluation of Carcinogenic Risks to Humans, 60*, 389–433.

Karsauliya, K., Yahavi, C., Pandey, A., Bhateria, M., Sonker, A. K., Pandey, H., Sharma, M., & Singh, S. P. (2022). Co-occurrence of mycotoxins: A review on bioanalytical methods for simultaneous analysis in human biological samples, mixture toxicity and risk assessment strategies. *Toxicon, 218*, 25–39. https://doi.org/10.1016/j.toxicon.2022.08.016

Kemboi, D. C., Ochieng, P. E., Antonissen, G., Croubels, S., Scippo, M.-L., Okoth, S., … Gathumbi, J. K. (2020). Multi-mycotoxin occurrence in dairy cattle and poultry feeds and feed ingredients from Machakos Town, Kenya. *Toxins, 12*, E762. https://doi.org/10.3390/toxins12120762

Knutsen, H. K., Alexander, J., Barregård, L., Bignami, M., Brüschweiler, B., Ceccatelli, S., … Edler, L. (2017). Risks to human and animal health related to the presence of deoxynivalenol and its acetylated and modified forms in food and feed. *EFSA Journal, 15*, Article e04718. https://doi.org/10.2903/j.efsa.2017.4718

Kopp, B., Vignard, J., Mirey, G., Fessard, V., Zalko, D., Le Hgarat, L., & Audebert, M. (2018). Genotoxicity and mutagenicity assessment of food contaminant mixtures present in the French diet. *Environmental and Molecular Mutagenesis, 59*, 742–754. https://doi.org/10.1002/em.22214

Luo, S., Terciolo, C., Neves, M., Puel, S., Naylies, C., Lippi, Y., … Oswald, I. P. (2021). Comparative sensitivity of proliferative and differentiated intestinal epithelial cells to the food contaminant, deoxynivalenol. *Environmental Pollution, 277*, Article 116818. https://doi.org/10.1016/j.envpol.2021.116818

Ma, Z., He, Y., Li, Y., Wang, Q., Fang, M., Yang, Q., … Xu, L. (2024). Effects of deoxynivalenol and its acetylated derivatives on lipid metabolism in human normal hepatocytes. *Toxins, 16*, 294. https://doi.org/10.3390/toxins16070294

McCarthy, D. J., Chen, Y., & Smyth, G. K. (2012). Differential expression analysis of multifactor RNA-Seq experiments with respect to biological variation. *Nucleic Acids Research, 40*, 4288–4297. https://doi.org/10.1093/nar/gks042

Mei, N., Guo, L., Tseng, J., Dial, S. L., Liao, W., & Manjanatha, M. G. (2008). Gene expression changes associated with xenobiotic metabolism pathways in mice exposed to acrylamide. *Environmental and Molecular Mutagenesis, 49*, 741–745. https://doi.org/10.1002/em.20429

Namorado, S., Martins, C., Ogura, J., Assunção, R., Vasco, E., Appenzeller, B., … Alvito, P. (2024). Exposure assessment of the European adult population to deoxynivalenol – Results from the HBM4EU aligned studies. *Food Research International, 198*, Article 115281. https://doi.org/10.1016/j.foodres.2024.115281

Palus, K. (2024). Dietary exposure to acrylamide has negative effects on the gastrointestinal tract: A review. *Nutrients, 16*, 2032. https://doi.org/10.3390/nu16132032

Payros, D., Dobrindt, U., Martin, P., Secher, T., Bracarense, A. P. F. L., Boury, M., … Oswald, I. P. (2017). The food contaminant deoxynivalenol exacerbates the genotoxicity of gut microbiota. *mBio, 8*, e00007–e00017. https://doi.org/10.1128/mBio.00007-17

Pestka, J. J. (2008). Mechanisms of deoxynivalenol-induced gene expression and apoptosis. *Food Additives & Contaminants: Part A: Chemistry, Analysis, Control, Exposure & Risk Assessment, 25*, 1128–1140. https://doi.org/10.1080/02652030802056626

Pinton, P., & Oswald, I. P. (2014). Effect of deoxynivalenol and other type B trichothecenes on the intestine: A review. *Toxins, 6*, 1615–1643. https://doi.org/10.3390/toxins6051615

Pons, B. J., Pettes-Duler, A., Naylies, C., Taieb, F., Bouchenot, C., Hashim, S., … Vignard, J. (2021). Chronic exposure to cytolethal distending toxin (CDT) promotes a cGAS-dependent type I interferon response. *Cellular and Molecular Life Sciences, 78*, 6319–6335. https://doi.org/10.1007/s00018-021-03902-x

R Core Team (2022). R: A language and environment for statistical computing. R Foundation for Statistical Computing, Vienna, Austria. URL http://www.R-project.org.

Ribet, L., Kassis, A., Jacquier, E., Monnet, C., Durand-Dubief, M., & Bosco, N. (2024). The nutritional contribution and relationship with health of bread consumption: A narrative review. *Critical Reviews in Food Science and Nutrition, 1–28*. https://doi.org/10.1080/10408398.2024.2428593

Rifai, L., & Saleh, F. A. (2020). A review on acrylamide in food: Occurrence, toxicity, and mitigation strategies. *International Journal of Toxicology, 39*, 93–102. https://doi.org/10.1177/1091581820902405

Robinson, M. D., McCarthy, D. J., & Smyth, G. K. (2010). edgeR: A bioconductor package for differential expression analysis of digital gene expression data. *Bioinformatics, Oxf. Engl., 26*, 139–140. https://doi.org/10.1093/bioinformatics/btp616

Rogakou, E. P., Nieves-Neira, W., Boon, C., Pommier, Y., & Bonner, W. M. (2000). Initiation of DNA fragmentation during apoptosis induces phosphorylation of H2AX histone at serine 139*. *The Journal of Biological Chemistry, 275*, 9390–9395. https://doi.org/10.1074/jbc.275.13.9390

Rogakou, E. P., Pilch, D. R., Orr, A. H., Ivanova, V. S., & Bonner, W. M. (1998). DNA double-stranded breaks induce histone H2AX phosphorylation on serine 139. *The Journal of Biological Chemistry, 273*, 5858–5868. https://doi.org/10.1074/jbc.273.10.5858

Sarion, C., Codină, G. G., & Dabija, A. (2021). Acrylamide in bakery products: A review on health risks, legal regulations and strategies to reduce its formation. *International Journal of Environmental Research and Public Health, 18*, 4332. https://doi.org/10.3390/ijerph18084332

Shiraishi, Y. (1978). Chromosome aberrations induced by monomeric acrylamide in bone marrow and germ cells of mice. *Mutation Research, Fundamental and Molecular Mechanisms of Mutagenesis, 57*, 313–324. https://doi.org/10.1016/0027-5107(78)90216-6

Song, D., Xu, C., Holck, A. L., & Liu, R. (2021). Acrylamide inhibits autophagy, induces apoptosis and alters cellular metabolic profiles. *Ecotoxicology and Environmental Safety, 208*, Article 111543. https://doi.org/10.1016/j.ecoenv.2020.111543

Takakura, N., Nesslany, F., Fessard, V., & Le Hegarat, L. (2014). Absence of in vitro genotoxicity potential of the mycotoxin deoxynivalenol in bacteria and in human TK6 and HepaRG cell lines. *Food and Chemical Toxicology, 66*, 113–121. https://doi.org/10.1016/j.fct.2014.01.029

Thielecke, F., & Nugent, A. P. (2018). Contaminants in grain—A major risk for whole grain safety? *Nutrients, 10*, 1213. https://doi.org/10.3390/nu10091213

Wang, A., Chen, X., Wang, L., Jia, W., Wan, X., Jiao, J., Yao, W., & Zhang, Y. (2022). Catechins protect against acrylamide- and glycidamide-induced cellular toxicity via rescuing cellular apoptosis and DNA damage. *Food and Chemical Toxicology, 167*, Article 113253. https://doi.org/10.1016/j.fct.2022.113253

Wang, S., Wu, K., Xue, D., Zhang, C., Rajput, S. A., & Qi, D. (2021). Mechanism of deoxynivalenol mediated gastrointestinal toxicity: Insights from mitochondrial dysfunction. *Food and Chemical Toxicology, 153*, Article 112214. https://doi.org/10.1016/j.fct.2021.112214

Waterman, D. P., Haber, J. E., & Smolka, M. B. (2020). Checkpoint responses to DNA double-strand breaks. *Annual Review of Biochemistry, 89*, 103–133. https://doi.org/10.1146/annurev-biochem-011520-104722

Weaver, A. C., Weaver, D. M., Adams, N., & Yiannikouris, A. (2021). Co-occurrence of 35 mycotoxins: A seven-year survey of corn grain and corn silage in the United States. *Toxins, 13*, 516. https://doi.org/10.3390/toxins13080516

Willoquet, B., Mirey, G., Labat, O., Garofalo, M., Puel, S., Penary, M., Soler, L., Vettorazzi, A., Vignard, J., Oswald, I. P., & Payros, D. (2024). Roles of cytochromes P450 and ribosome inhibition in the interaction between two preoccupying mycotoxins, aflatoxin B1 and deoxynivalenol. *Science of the Total Environment, 955*, Article 176937. https://doi.org/10.1016/j.scitotenv.2024.176937

Yan, F., Wang, L., Zhao, L., Wang, C., Lu, Q., & Liu, R. (2023). Acrylamide in food: Occurrence, metabolism, molecular toxicity mechanism and detoxification by phytochemicals. *Food and Chemical Toxicology, 175*, Article 113696. https://doi.org/10.1016/j.fct.2023.113696

Yousef, M. I., & El-Demerdash, F. M. (2006). Acrylamide-induced oxidative stress and biochemical perturbations in rats. *Toxicology, 219*, 133–141. https://doi.org/10.1016/j.tox.2005.11.008

Zhang, J., Zhao, Q., Xue, Z., Zhang, S., Ren, Z., Chen, S., … Liu, Y. (2023). Deoxynivalenol induces endoplasmic reticulum stress-associated apoptosis via the IRE1/JNK/CHOP pathway in porcine alveolar macrophage 3D4/21 cells. *Food and Chemical Toxicology, 180*, Article 114033. https://doi.org/10.1016/j.fct.2023.114033

Zhang, X., Jiang, L., Geng, C., Cao, J., & Zhong, L. (2009). The role of oxidative stress in deoxynivalenol-induced DNA damage in HepG2 cells. *Toxicon, 54*, 513–518. https://doi.org/10.1016/j.toxicon.2009.05.021

Zhang, Y., Ouyang, B., Zhang, W., Guang, C., Xu, W., & Mu, W. (2024). Deoxynivalenol: Occurrence, toxicity, and degradation. *Food Control, 155*, Article 110027. https://doi.org/10.1016/j.foodcont.2023.110027

Zhao, L., Zhang, L., Xu, Z., Liu, X., Chen, L., Dai, J., … Sun, L. (2021). Occurrence of aflatoxin B1, deoxynivalenol and zearalenone in feeds in China during 2018–2020. *Journal of Animal Science and Biotechnology, 12*, 74. https://doi.org/10.1186/s40104-021-00603-0

Zhou, Y., Zhou, B., Pache, L., Chang, M., Khodabakhshi, A. H., Tanaseichuk, O., … Chanda, S. K. (2019). Metascape provides a biologist-oriented resource for the analysis of systems-level datasets. *Nature Communications, 10*, 1523. https://doi.org/10.1038/s41467-019-09234-6